ELECTRONIC PROPERTIES OF SURFACE NANOFEATURES ON ZINC OXIDE

Senior Honors Thesis

Presented in Partial Fulfillment of the Requirements for
Graduation with Honors and Distinction in the
College of Engineering of The Ohio State University

By

Timothy S. Bolton

* * * * *

The Ohio State University

2010

Honors Thesis Committee:

Dr. Leonard Brillson, Adviser

Dr. Paul Berger

ABSTRACT

Zinc Oxide undergoes spontaneous nano-sized feature growth in ambient conditions. These features are both physical and electronic characteristics that are measurable with nanometer-resolution techniques such as atomic force microscopy, Kelvin probe force microscopy, surface photovoltage spectroscopy, and cathodo-luminescence spectroscopy. Two defects, zinc vacancy and oxygen vacancy, are associated with these nanofeatures both at the surface and below the surface. It was found that the face polarity (Zn face or O face) affects the growth of nanofeatures in several different ways: which feature is most commonly seen (rod on O, pit on Zn), whether rosette features radiate above-surface lines or trenches (above on O, trenches on Zn), and the dominating defect (O vacancies on zinc face, Zn vacancies on O). The hexagonal close-packed crystal structure of ZnO propagates to feature growth, seen by the clearly-defined hexagonal shape of pits on zinc face, by the rosette projection lines at angle multiples of 60º, and trench lines bending at multiples of 60º. In many cases, there is a strong correlation between surface topography of features and surface potential which indicates surface states, with continued (and new) growth along those states; the lack of KPFM correlation alludes to subsurface states.

ACKNOWLEDGMENTS

Thanks to my adviser, Dr. Leonard Brillson, whose intelligence and charisma have been instrumental in my pursuit of this undergraduate research and the compilation of this thesis, as well as The Ohio State University for a scholarship grant to pursue this. Thanks to the great group of researchers under Dr. Brillson who gave me encouragement and aid, most especially: Tyler Merz, Daniel Doutt, Yufeng Dong, Evan Katz, and Chung-Han Lin. Finally, thanks to my family and friends who have, as always, supported me—especially Jeremiah Santos for his reviewing aid.

VITA

1987 . . . . . Born

March, 2010 . . . . . B.S. Electrical & Computer Engineering
The Ohio State University
Columbus, Ohio

FIELDS OF STUDY

Major Field: Electrical Engineering

Studies in:

Electromagnetism
Power Systems
Solid-State Electronics

TABLE OF CONTENTS

Page

LIST OF FIGURES

CHAPTER 1

INTRODUCTION

Day after day, electronics become increasingly more integrated in our lives as the technologies continue to improve. Consumers (e.g. industry, civilians, military, etc.) demand higher efficiency, lower cost, smaller size, and increased functionality from the next wave of electronics. Yet there are both theoretical and practical limits to this: electronics materials have theoretical limits due to their properties, with modern technology defining the practical limit of tapping the material's full potential. Materials research, then, is essential to pushing forward.

Silicon has been, and continues to be, a fantastic material that has scaled well over the years since electronics' inception in the mid-1900s, enabling the creation of innumerable different types of devices. Other materials have been extensively researched as well, in the goal of discovering their theoretical and practical limits. Some have been entered the commercial fray due to advancements, while many continue to be constrained to niche markets—unlocking their tantalizing properties continues to require tremendous effort that is not yet economically viable until more advancements have been made. Zinc oxide is an example of the latter.

1.1 Motivation

Zinc oxide (ZnO) is one of many compound semiconductor materials useful for electronics of various types. Among those uses are: optoelectronics in the blue to near-UV spectrum, transparent electronics, spintronics, piezo-electronics, and gas sensors. ZnO's bandgap is near 3.4 eV (room temperature), which is in the near-UV spectrum and therefore transparent. The lattice constants are: a = 3.25 Å and c = 5.2 Å. It also is a direct-gap material, and it is characterized as a hexagonal close-packed (HCP) structure.

Another strength of ZnO is its abundance. Zinc is a very common material, and ZnO is used a variety of products such as suntan lotion, paint, galvanization, and more recently, thin-film photovoltaics. This is a huge boon for transparent conducting oxides (TCOs) because the nominal material, indium tin oxide, is limited somewhat due to the low abundance of Indium and high price. Add the facts that ZnO is inert (even safe to consume) and is radiation-hard, and it is easy to see why ZnO is so attractive.

As mentioned before, ZnO still has weaknesses holding it back. Chief among those is the inability to create a stable and reproducible p-type ZnO by doping, in some part due to compensation by the intrinsic ZnO donor states. Therefore ZnO is intrinsically n-type. This is debilitating as far as electronics are concerned: the usage of both p-type and n-type regions is key to produce a p-type transistor or a diode, the common semiconductor devices. Hall mobilities upwards of 3100 $cm^2V^{-1}s^{-1}$ have been reported for electrons, while hole mobilities are closer to 5-30 $cm^2V^{-1}s^{-1}$—significantly slower [1].

Research into p-type doping is on-going, as are ZnO's other properties. Much of

such research has been on the bulk properties of ZnO, while the surface properties have been ignored. That the surface layer is important may be surprising at first, but it shouldn't be: it plays a role as an interface between the bulk ZnO and the deposited device. It also plays a role in the growth of nanostructures—the growth methods, properties, and uses of it—which have been increasingly researched. Understanding the surface properties of ZnO, then, leads to comprehending its behavior as an interface or for growing nanostructures and the appropriate ways for exploiting it.

1.2 History

This research is a subset of the ongoing research being pursued by The Ohio State University's Electronic Materials and Nanostructures Laboratory. Previous work has gone into exploring the electronic properties of surface nanofeatures on ZnO by researchers Yufeng Dong, Daniel Doutt, and Tyler Merz under Dr. Brillson.

One piece of work that couples the importance of surface nanofeatures with a macro-scale description is that of surface roughness. The effect of surface roughness was thoroughly explored. Doutt, *et al.* prepared multiple ZnO samples and performed a variety of tests [2]. One test was to compare the surface morphology (see Fig. 10, left) with the corresponding spatial potentials (Fig. 1, right) for a high-defect (Hydrothermal-16) and low-defect (Hydrothermal-1) ZnO sample. For the high-defect sample, the surface pits generally had corresponding potential change regions and some lateral regions of flat potential, indicating some surface defect dependence along with some subsurface defects; for the low-defect sample, the pits did not generally correspond to regions of potential

change—therefore, the pits formed due to subsurface defects which was not seen by the KPFM at the surface.

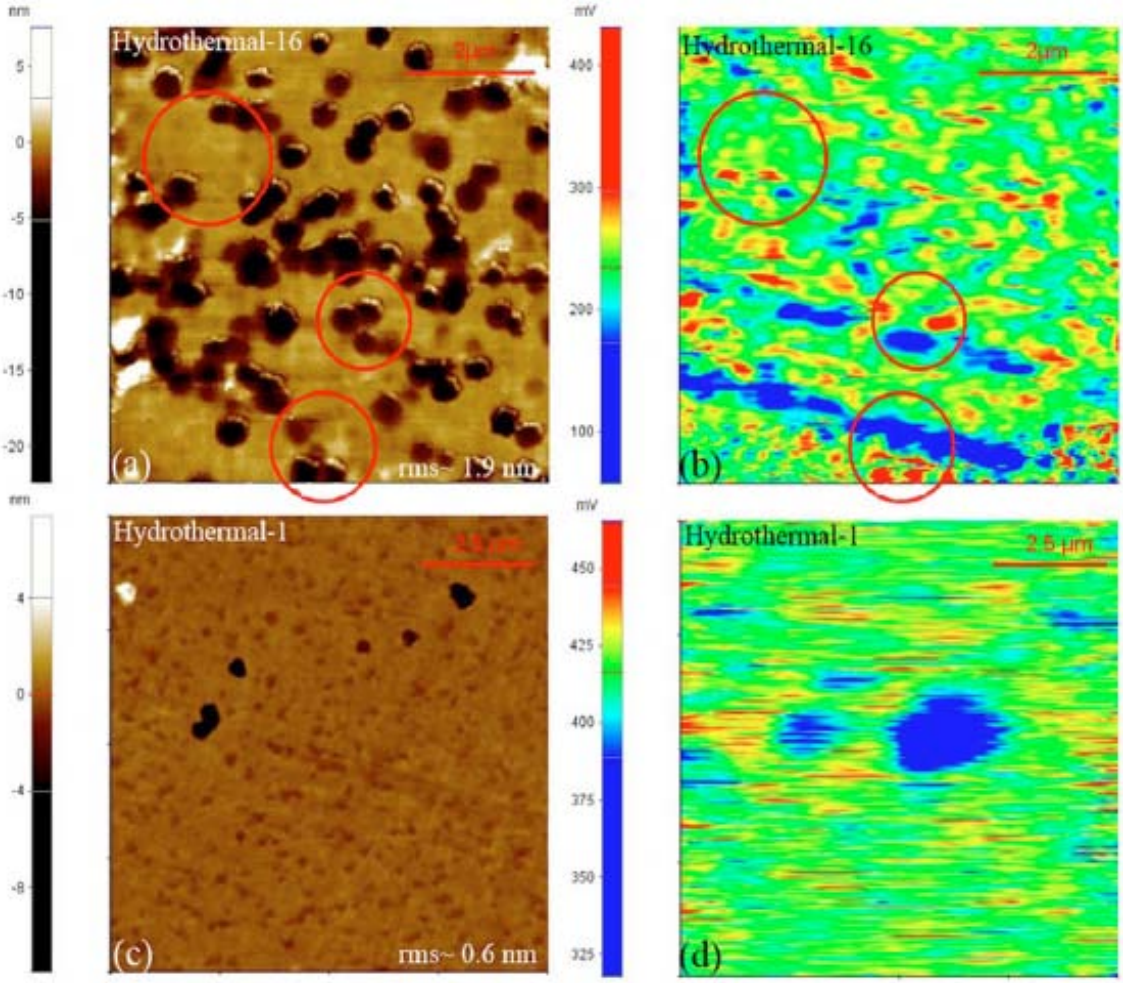

Figure 1 – ZnO Morphology and Potential Plots (Left: AFM; Right: KPFM) [2]

Another test was done on surface roughness for multiple surfaces to characterize their DR-CLS (see section 3.4) subsurface intensity efficiency (near-band edge emissions divided by defect peak emissions) (see Fig. 2) [2]. From the exponential decay fit curve, the surface roughness significantly affects UV output efficiency, sharply increasing for average roughnesses less than 0.5 nanometers. This average roughness to efficiency correlation stems from the roughness being less than the ZnO unit cell dimension (0.52

nm), indicating lattice imperfections are the cause for the extreme decline in UV output efficiency. Forming consistent, perfect lattice structures would be a pivotal breakthrough and is worthy of research.

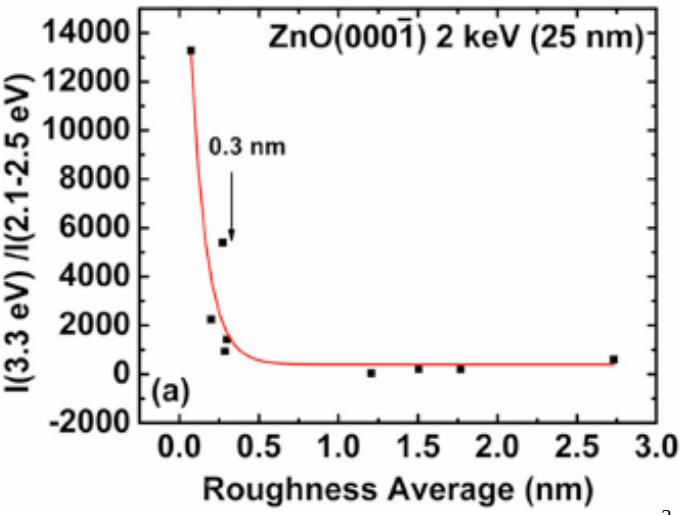

Figure 2 – ZnO CLS Intensity vs. Surface Roughness [2]

The above surface roughness work uses some of the same measurement techniques used in this paper. Its results help to re-iterate how important a semiconductor's surface is, showing why more research is necessary to understand and control any surface phenomena.

1.3 Organization of Thesis

The remainder of this thesis is divided into the following chapters. Chapter Two describes the background information surrounding zinc oxide nanofeatures and surface defect states. Chapter Three introduces the concepts behind the measurement techniques employed. Chapter Four presents research results and discusses them. Finally, Chapter Five draws conclusions on the research and discusses future concepts for exploration.

CHAPTER 2

ZINC OXIDE BACKGROUND INFORMATION

In this section, information pertaining to zinc oxide nanofeatures and defect states are presented in small detail. This knowledge is necessary to comprehend the results obtained and explained in chapter four.

2.1 Surface Nanofeatures

Researchers have poured intensive effort into forming a variety of geometric structures on semiconductors, such as rings, wires, rods, tips, and pyramids. Some of these can involve very complex processes, requiring great control of parameters for desired growth. Yet, interestingly enough, ZnO naturally and spontaneously grows its own nanofeatures: pits, rods/bumps, and rosettes.

Of these natural features, it is only the rosette that is not intuitive. Pits and rods/bumps are just as they sound—pits are holes in the surface, and can have hexagonal edges; rods/bumps grow on the surface and can look like a rod or a bump depending on the height of the structure and its diameter. Rosettes are pits with a twist: topographical lines project from these pits, either from the hexagonal pit vertices or normal to the

hexagonal sides, and can be either raised or trench lines. The size of these features can range from less than a nanometer (such as rosette line heights) to several hundred nanometers in height/depth to the surface or to several microns in diameter. Again, these features grow spontaneously in ambient conditions—room temperature and air exposure. And, as will be discussed, these features grow in different patterns depending on the surface face polarity.

Yet another feature which can be observed is islanding. These islands form on the ZnO surface in random patterns across the surface, in ways that are not yet fully understood. They were seen on a sample that had undergone annealing in an oxygen plasma, which would have both cleaned the surface and made it more reactive.

2.2 Vacancy Defect States

As was mentioned previously, ZnO's bandgap is around 3.4 eV at room temperature. Two other energies are important, especially in the context of this paper: 2.1 eV and 2.45 eV. These represent zinc and oxygen vacancies, respectively, which play an important role in surface nanofeatures, among other things.

The zinc vacancy state is located around 2.1 eV below the conduction band and is just that: an atomic lattice site vacancy where a zinc atom is expected. It is p-type in character, therefore an acceptor. Dong has showed, however, that isolated zinc vacancies can show effects at lower energies than 2.1 eV [3].

Similarly, the oxygen vacancy state is located around 2.45 eV above the valence band. It is n-type in character, therefore acting like a donor. Its energy state, too, isn't necessarily pinned at 2.45 eV—it can be around 2.4 – 2.6 eV [3].

CHAPTER 3

MEASUREMENT TECHNIQUES USED

Acquiring data is integral to modern research. While many differing approaches are of tremendous gain in the examination of ZnO to understand its nanoscale properties, three particular techniques are of great import: atomic force microscopy (AFM), Kelvin probe force microscopy (KPFM), surface photovoltage spectroscopy (SPS/SPV), and depth-resolved cathodoluminescence spectroscopy (DR-CLS). The AFM and KPFM are taken simultaneously over a large area, while the SPS and DR-CLS are taken separately at desired points. The following sections expand upon each of these techniques, including their theory and their relevance in this research.

3.1 Atomic Force Microscopy (AFM)

This technique's usefulness includes quantization of “surface topography, elasticity, friction, adhesion, charge density, magnetic structure, or even long-range effects” and more [4]. Four different modes exist: contact mode, non-contact mode, tapping mode, and scanning capacitance microscopy (SCM). These techniques were historically slow due to the raster speed across the sample and had poor resolution, but

both have increased dramatically since AFM's inception in 1986.

Various industries use AFM in their research. Biology, for example, would find these techniques useful in imaging the make-up (see Figure 3, left), mechanical, and chemical properties of cellular structures. The photonics and semiconductor industries also rely heavily on AFM (see Fig. 3, right) to map and characterize the atomic structure of processed materials, such as wafers and deposition processes, which provides critical information necessary for optimization and modification.

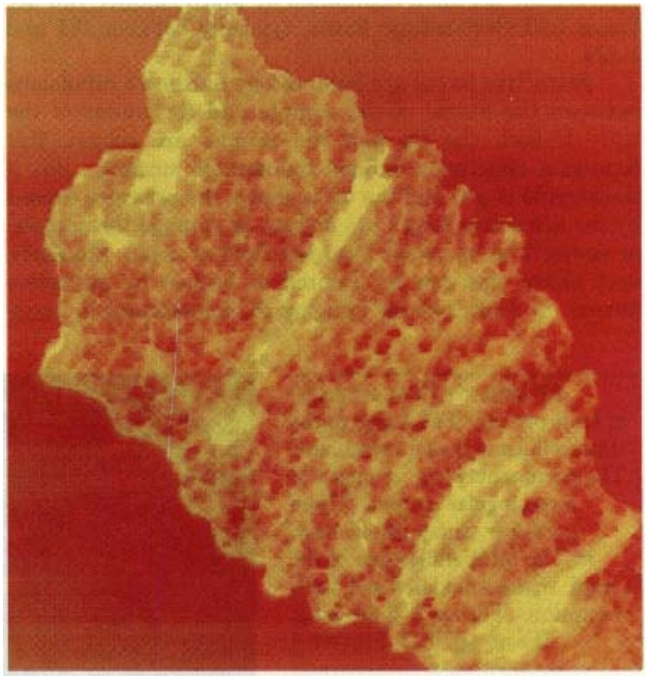

CONTACT-MODE IMAGE of a polytene chromosome from the salivary gland of the common fruit fly, obtained in air using a tip produced by electron-beam deposition. The width of the chromosome is about 6 microns. (From ref. 8, courtesy of Eric Henderson, Iowa State University.) FIGURE 2

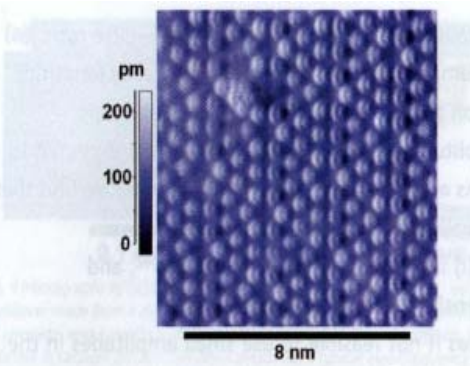

Fig. 5 AFM image of the Si 7×7 reconstruction with true atomic resolutio cantilever. Parameters: k = 1800 N/m; A = 0.8 nm; f_0 = 16.86 kHz; Δf = Q = 4000. Environment: ultrahigh vacuum, room temperature. (Reprinte from[51]. © 2000 AAAS.)

Figure 3 – Example Biological AFM Image [5] (left) and Example Si AFM [6] (right)

Contact mode analysis is the basis for the beginning of AFM. In this mode, the probe tip of the AFM machine is “scraped” across the sample as it is raster-scanned. This can be used to generate various information, excluding long-range force effects.

However, scraping a tip across a sample's surface can damage the tip in addition to the surface, nullifying reproducibility; this is an unwanted side-effect, among others, which is addressed by the non-contact and tapping modes [5]. In contact-mode, as the probe tip is raster-scans across, the tip experiences compression and shear forces. Eventually the tip will break or be blunted; this is unavoidable, but at some level, there is a trade-off between accuracy (tip sharpness) and reliability.

Several techniques are used for the deflection detection, but the most common is that of an optical beam [5]. By mounting a laser and reflecting it off of the cantilever into a photo-detector, the optical beam's deflection can be measured. Using known equations and relations, the cantilever's deflection can be computed and recorded. The gain factor using this method is high, being usually in the range of 300-1000, allowing for very accurate measurement data to be taken. Because of this, detecting the deflection is straightforward; in fact, deflection resolution is around 0.01 nanometers (sub-Angstrom).

For illustration of this mode, see Figure 4. As seen, it is the sample that is moved, not the tip; to do otherwise would pose significant accuracy and reproducibility challenges. The tip is then scraped across the surface; as the tip is moved up and down throughout its journey, the deflection of the cantilever, upon which the tip is mounted, is measured and recorded. If the probe tip is one atom thick at the very apex, then the tip is literally scanning individual atoms. These deflections give rise to atomic topography information, allowing for an image such as seen in Figure 3 to be created.

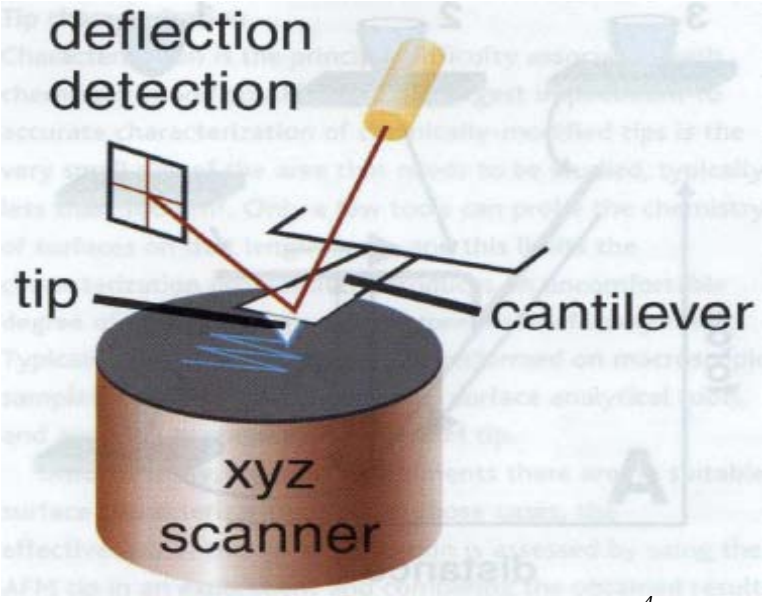

Figure 4 – Contact Mode Illustration [4]

More than a sample's physical characteristics can be explored by using a conducting tip, such as measuring voltage potential (giving rise to KPFM), current, or resistivity at specific points. For example, a group of researchers used AFM with a conducting tip in contact mode to analyze a laser's internal efficiency [7]. By applying a measurable forward current on the sample, the tip was able to measure the local resistivity across the surface—from this, the voltage could be determined. After this investigation of the voltage drop across specific layer regions, the researchers estimated that approximately forty percent of injected current was being wasted inside the laser device.

Non-contact mode is what it implies: the probe tip is always kept at a distance from the sample being measured, typically a few nanometers [5]. This can be used for measuring electrostatic force, charge density, magnetic structure, short-range chemical forces, and surface topography. Unfortunately, because the tip is kept at a distance from

the sample, applying a buffer solution on top of the sample will blur the force interaction on the probe tip. For this reason, biological testing does not usually employ this method.

Non-contact employs frequency modulation [6]. Just as is implied, the cantilever is vibrated at a constant frequency which is mathematically derived, usually around 100 kilohertz to one megahertz [5]. This frequency, called the eigenfrequency, is derived from the mass and stiffness of the cantilever [6]. Using this, any changes to the frequency of the probe tip as it is raster-scanned across the sample will be measured and analyzed; if this frequency change is not constant, though, mathematical complications arise. The frequency change can be varying in orders of magnitude; it is caused by a force gradient between the sample and tip.

Tapping mode can be best described as a compromise between the contact and non-contact modes [5]. It employs characteristics from both—the tip is oscillated at a frequency, but makes contact with the sample at the bottom of its rotation. Its use, though, is geared more towards the contact-mode type, particularly surface topography, elasticity, and adhesiveness [8].

The AFM results gathered in this report employ non-contact mode. This is done to maximize tip life, minimize surface damage (and therefore maximize repeatability on that same area), and enable KPFM. In this manner, strong results are attained with the exception of any microscopic dirt on the sample--this will appear as a bump, rod, or cluster on the surface depending on the geometry. Using this AFM mode, tip life was long and topography maps were consistently repeatable.

3.2 Kelvin Probe Force Microscopy (KPFM)

KPFM is a method for measuring the surface potential on a sample. This can be achieved with an AFM and a conductive tip. What is special about this method is that it makes a parallel capacitor between the tip and surface—thus a non-contact mode of microscopy [9]. Because the cantilever is vibrated at a set frequency, a measurable current is created in the tip as the distance between the tip and surface changes (and therefore the capacitance); this current is nullified by applying a DC bias. Unfortunately, this method is not as spatially-resolved as other techniques, due to interaction from a small surface area beneath the tip--not just the point directly beneath the tip.

For common use with an AFM, an AC voltage needs to be applied between the tip and sample[9]. Knowing the AC voltage, resonance frequency, and distance from the sample, the contact potential difference (between the tip and sample) can be deduced from the electrostatic force interaction upon the tip, which is measured (see Fig. 5). This is a relatively straightforward modification of an AFM, allowing both topography and surface potential to be measured simultaneously, allowing for meaningful correlation between surface features physical and electronic attributes.

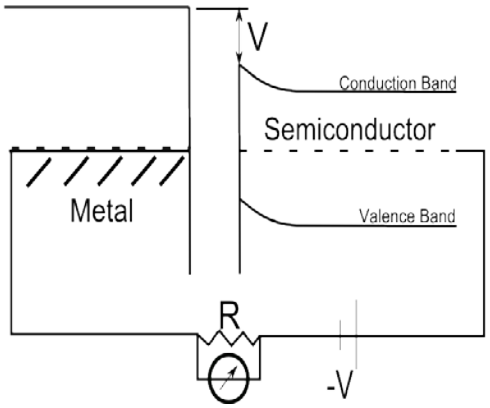

Figure 5 – KPFM Band Diagram (tip on left, sample on right) [by Tyler Merz]

3.3 Surface Photovoltage Spectroscopy (SPS/SPV)

The goal of SPS is to gather information about a material's surface (and near-surface) response to changing impinging energies of light, by virtue of measuring the surface potential. It is useful as a tool for "linking the physics, chemistry, and electrical performance of semiconductors" [10]. This technique is easy to implement by coupling an AFM using the KPFM technique with a variable light source (such as an adjustable-wavelength monochromator). This technique can be slow, though, to allow for carrier lifetimes to decay, which is important.

The theory behind SPS lies with the surface photovoltage effect: incident photons will generate electron transitions if they supersede the bandgap—or if they supersede the difference between a trap (or defect) and either the conduction or valence band. As incident light stimulates transitions at the surface and near-surface due to defect (or impurity) sites or the bandgap, the built-in voltage across the surface charge region will be affected [10]. This can be measured and plotted as a function of wavelength energy; slope changes in the plotted curve will indicate the energy level of these sites (see Fig. 6 as an example). Negative slope changes indicate a transition of electrons from a surface state to the conduction band from a donor state (flattening of band diagram); vice versa for holes transition from the valence band to a surface state as indicated by a positive slope change (acceptor state, sharpening of band).

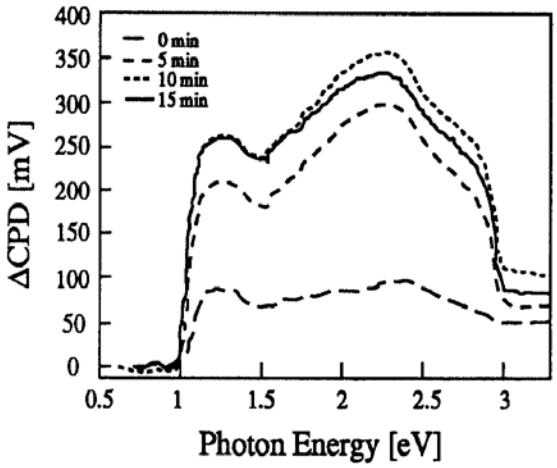

Figure 6 – SPS of a Multi-layer Semiconductor [10]

This technique, then, is useful in finding surface and sub-surface states in a sample. Normally this spectra is ascertained at a point and is very informative of the states associated at that area influencing the cantilever and tip, but can be difficult to be repeatable due to tip drift between and during scans. On-going work by Tyler Merz is expanding the technique to be spatially resolved at specific light wavelengths, because the light incident on the sample is larger than the scan area.

3.4 Depth-Resolved Cathodoluminescence Spectroscopy (DR-CLS)

This technique provides similar results to SPS, in that it generates a spectrum that identifies energy states of defects and their relative quantity in the sample at that point. It achieves it in a different manner, however, than SPS: a beam of electrons is directed onto the sample; these electrons will create photons at sufficient energies, which are collected by a monochromatic spectrum analyzer. The electron beam is varied in individual electron energies, to go over the range from 0 eV past bandgap. A trap or defect of a certain energy, then, will generate a photon when incident electrons have sufficient

energy to bridge from either the conduction band or valence band to the trap energy; these photons are then collected and analyzed (Fig. 7, middle and right).

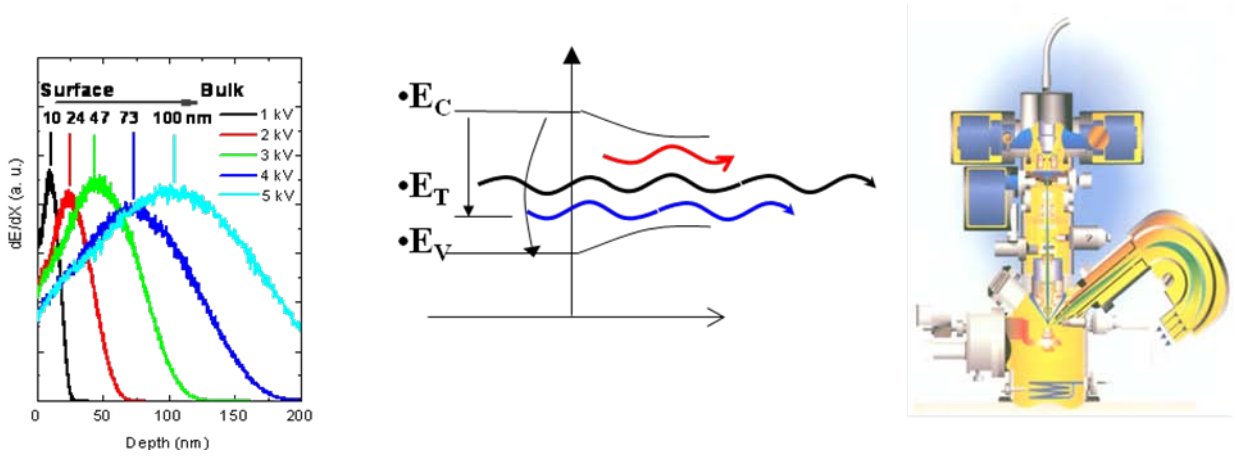

Figure 7 – DR-CLS Illustrations (left: Monte Carlo depth simulations; middle: band diagram of photon generation; right: equipment illustration) [by Yufeng Dong]

It is important to distinguish the energy of the individual electrons being beamed at the sample and the acceleration voltage used to create the beam. At increasing voltages, the electrons can be propelled further into the surface, revealing sub-surface states. However, the depth of surface penetration is statistic but random—Gaussian plots are generated by Monte Carlo simulations to estimate the statistical mean depth of a particular acceleration voltage (Fig 7, left). At very low voltages, such as less than one keV, this can be assumed to be very near (or at) the surface level.

CHAPTER 4

RESULTS

In this chapter, research results are presented. First, though, the equipment used and working conditions are described, then the samples used. Next, results from the O face are presented and followed by Zn face results, with some clear distinctions to be seen. Both faces exhibit nano-scale surface features, but in differing ways.

4.1 Experimental Procedure

Samples examined were grown by hydrothermal or vapor phase epitaxy (VPE) processes. Their surfaces were chemo-mechanically polished by their manufacturer. All substrates were subjected to a standard rinse for five minutes each in acetone, methanol, and de-ionized water, and then blown dry in nitrogen. All samples were undoped and are single crystalline. The first sample (sections 4.2 & 4.3) was grown by VPE; both Zn face (0001) and O face (000-1) opposing surfaces were polished. The second sample is also VPE, but was only polished on the Zn face; it has undergone oxygen plasma treatment. The third sample is grown hydrothermally, but has been polished on both sides. Samples 2 & 3 are only featured in Section 4.4 .

AFM, KPFM, and SPS were taken using a Park XE-70 atomic force microscope with relevant software and a Xe lamp source. All measurements were taken using a non-contact mode with an EFM (Electric Force Microscope) tip (AuCr or TiPit coated) with a curvature radius of less than 40 nm. All results were achieved in ambient conditions (room temperature, air), but measured in a vibration-controlled chamber to minimize fluctuations.

DR-CLS was taken using a JEOL 7800F ultrahigh vacuum scanning electron microscope (SEM). A parabolic mirror connected to a photomultiplier collected the luminescence. The sample was cooled with an Oxford stage using liquid He to a temperature of 10 K. An Oxford MonoCL monochromator was used to record the spectra with a maximum resolution of 0.15 nm. The SEM electron beam was varied with constant power from 0.2 to 1 keV with a maximum spot size of 50 nm. Spectra were taken at energies coinciding with surface states, as modeled by Monte Carlo simulations.

4.2 O Face

This face is characterized as being oxygen-terminated, that is, the last layer of crystal atoms at this surface are all oxygen. Oxygen atoms at polar surfaces have "dangling bonds" that are very reactive. They can react with ambient carbon and hydrogen species to form C-O and OH compounds. Also, O face seems to have more native defects than Zn face (Yufeng Dong via DR-CLS) as well as more impurities, suggesting that there is a possibility of surface segregation and electro-diffusion relevant to the oxygen terminating atoms [11]. The common nano-scale surface features can be

found on this face: pits, rods/bumps, and rosettes. As will be seen, nanorods tend to be more common on this face than pits, and can grow in alignment.

Nanorods (or bumps) grow in high density on ZnO. While they can certainly be randomly distributed, they can also be seen to grow in a line. This alignment typically parallels something happening electronically. Figure 8 shows this: on the left is an AFM map showing a line of nanorods (see circled area; note that white features correspond to above-surface, black to below-surface). These are termed "nanorods" since they have areal diameters on the surface that are much smaller than their heights perpendicular to the surface On the right of fig. 8 is a matching KPFM plot over exactly the same area which shows a line of negative potential (blue). This is very interesting; the nanorods prefer to grow along a defect line (whether the defects are at the surface or sub-surface), even though there is nothing topographically different about that region. It is likely that the nanorods along that KPFM line will continue to grow as well as new nanorods forming (some small ones can be seen). The KPFM is also more negative along this line where nanorods are present; this is because of defects forming at or under the surface.

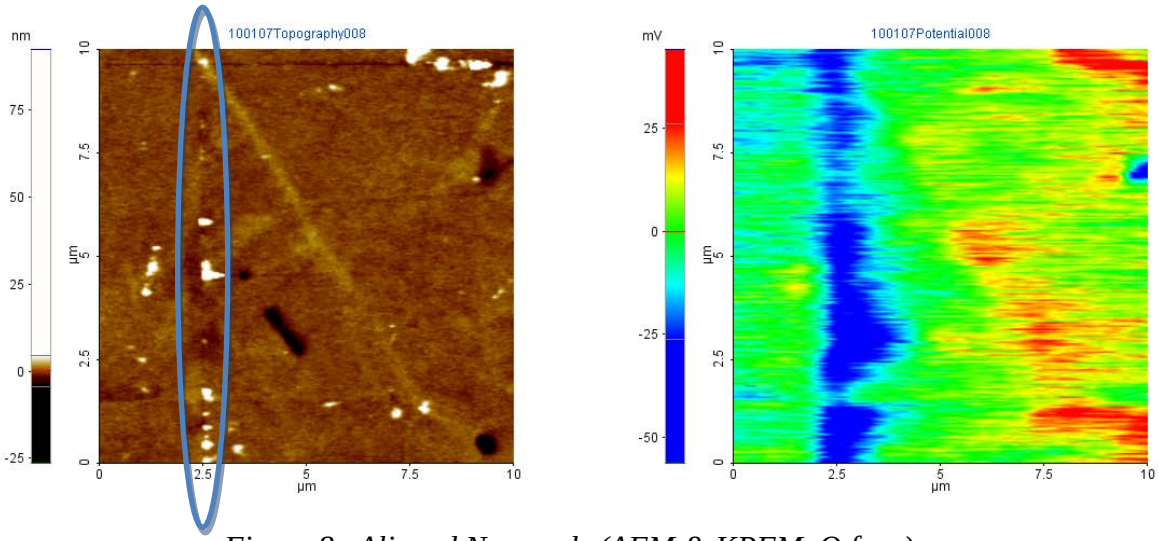

Figure 8 –Aligned Nanorods (AFM & KPFM, O face)

SPS plots taken around the above topography of aligned nanorods were not revealing. It was hoped to glean information regarding defect states comprising the potential line seen in Fig. 8. Figure 9(a) presents a morphology map of a ZnO O face. SPS spectra taken at points 1 through 4 appear in fig. 9(b). Note the strong peak around 3.4 eV; this is the near-band-edge response. Fig. 9 shows some of the points (2 – top of a rod and 3 – along the potential line) along the nanorod line exhibit weak positive slope changes around 2.1 eV, the energy corresponding to the zinc vacancy defect. Except for a distinct slope change at ~1.8 eV at point 1 and 2 eV at point 3, these are very slight, however, and barely rise out of the SPS noise.

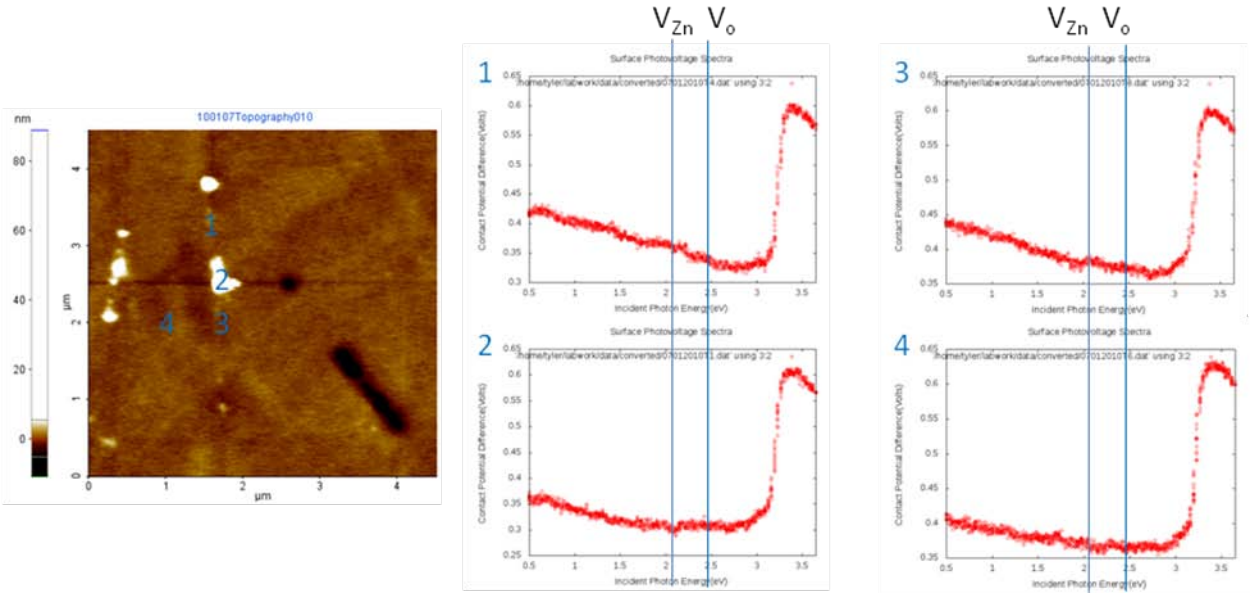

Figure 9 – Aligned Nanorods (AFM & SPS, O face)

Rosettes too have a link between AFM and KPFM. As described previously in this paper, rosettes are structures that involve a pit with lines radiating from it; these lines can emanate from the pit's vertices or side walls (usually difficult to discern on O face because pits are more circular) and can be either raised or lowered. Fig. 10 shows two

rosettes inter-connected by rosette lines (see left, circled pits) with matching KPFM signatures (see red lines on right-side map). Again, these potential lines indicate something important about surface and sub-surface states; however, SPS plots taken did not show anything conclusive. Note that rosette lines are approximately 120º apart—this is indicative of nanofeatures' tendency to exhibit hexagonal characteristics.

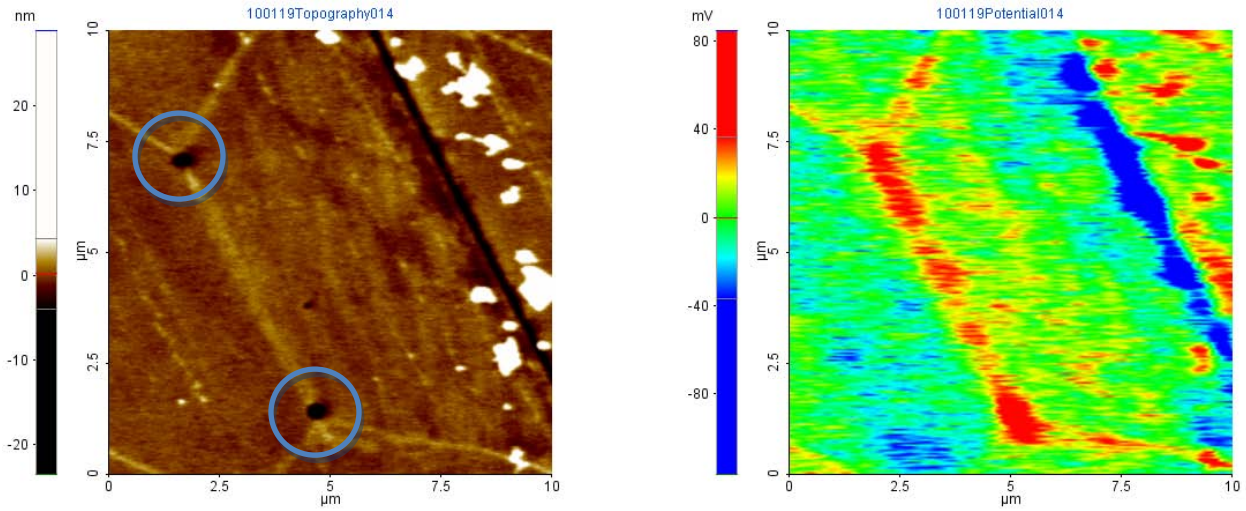

Figure 10 – Rosette (AFM & KPFM, O face)

Figure 11 showcases another rosette. This rosette has two projection lines from the pit at little less than 120º apart. The width of the rosette projection line is approximately 400 nm, and has a height of less than 1 nm (about two atomic monolayers). It is almost like a road or highway leading to/from the rosette: wide and shallow, it should be fairly easy for atoms to travel along. It has been conjectured by fellow researchers that these lines are pathways for zinc transport.

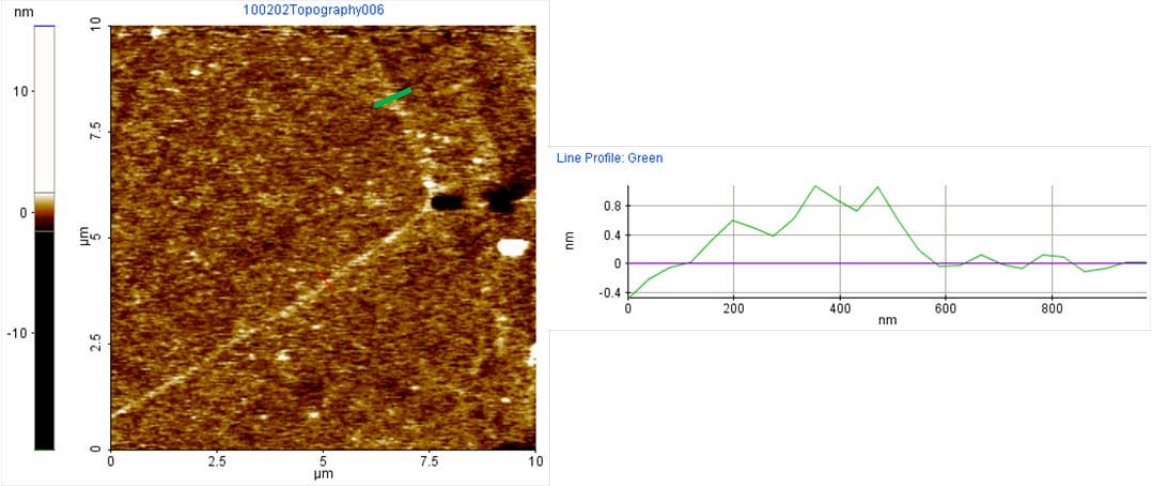

Figure 11 – Rosette Projection Line Profile (AFM, O face)

4.3 Zn Face

Conversely, this polar surface is characterized by being zinc-terminated. As mentioned in the previous section, this face has been found to possess significantly less defects and impurities. However, hydrogen diffuses and migrates along Zn face easier than on O face [12]. That said, all of the same features to be found on the O face can be found on the Zn face as well. In contrast to the O face, the Zn face tends to have aligned pits and rosette line trenches whereas O face surfaces have aligned nanorods and raised rosette lines.

Pits do indeed seem to be the common feature found on Zn face ZnO. Not only that, but they are distinctly hexagonal, as can be seen in Fig. 12. It is likely that these pits will continue to grow and merge together, forming a more uniform line. The KPFM potential correlates somewhat with the topography (hexagonal pits on left with red potential blotches on right). While features do typically have noticeable topographical and potential correlation, this figure (and others) indicates that not always does the

correlation exist strongly. This could be because of defects or impurities under the surface that change the potential.

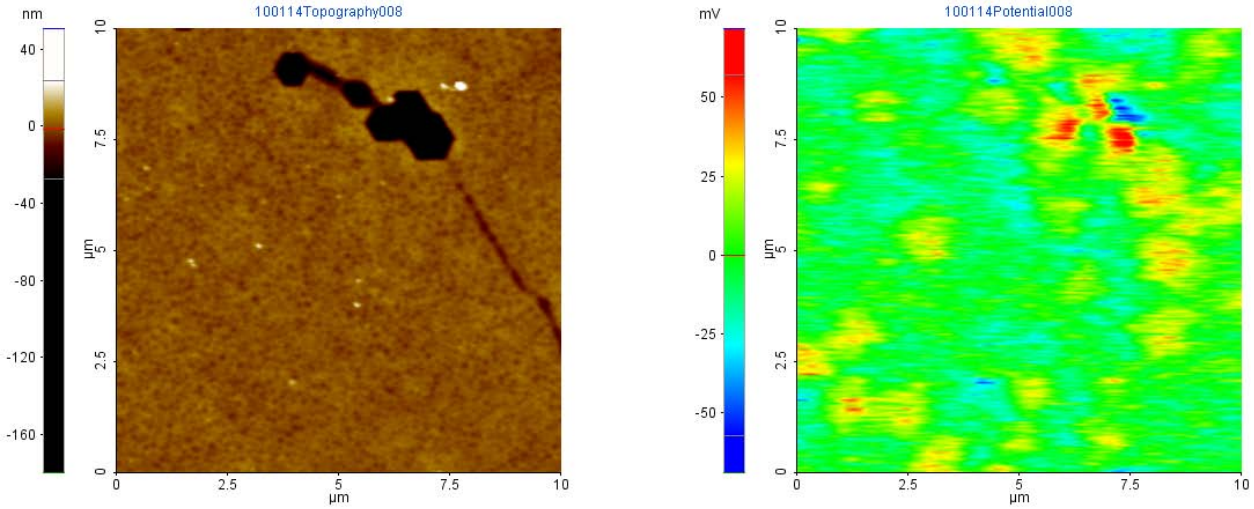

Figure 12 – Pit Line (AFM & KPFM, Zn face)

Rosettes are commonplace, too. Pictured below in Fig. 13 is a rosette of lines centered around and radiating away from a large pit, with pits and trenches radiating out from the center's sidewalls, separated by 120º. Only one of the projections (8 o'clock) correlates to the KPFM image (blue potential blotches), while the other two do not correlate. Strangely, the KPFM map indicates many electronic states around the surface (red and blue), but these do not correlate to any noticeable topography.

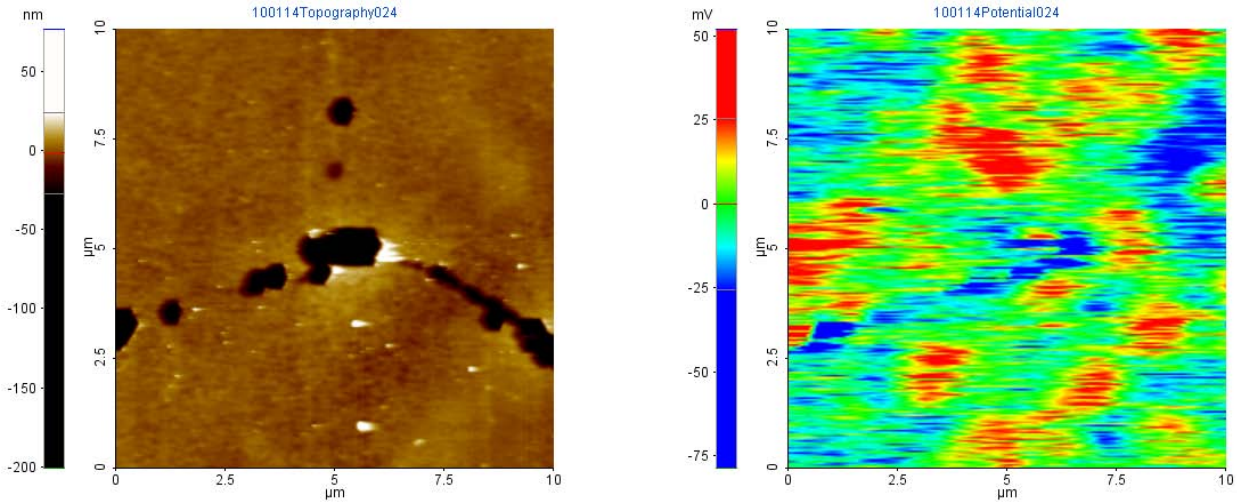

Figure 13 – Rosette (AFM & KPFM, Zn face)

Another rosette is pictured below in Fig. 14; this has the more commonly seen projection lines from the rosette—solid lines, not a collection of pits (as in Fig. 13). In this one, the projection lines emanate from the hexagonal pit's vertices. These two projection lines were measured: both are several nanometers in depth (less than ten atomic monolayers), and are several hundred nm in width—again, wide and shallow, making great pathways for atoms to move along, potentially. It is possible that Zn moved along these directions and depleted the lattice of Zn along this line, leaving only O which then evaporated—this would result in a "canyon" as seen.

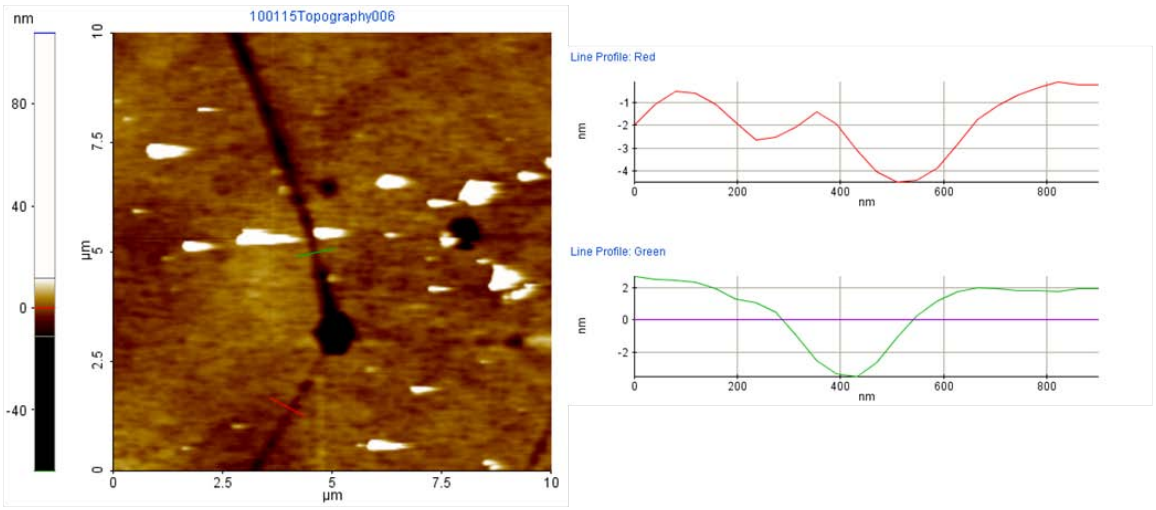

Figure 14 – Rosette Projection Line Profiles (AFM, Zn face)

The number of rosette projection lines angling from a pit can vary from 1 to 6, the number of faces or corners in a hexagon. A great AFM plot was taken that shows the strong 60º line intervals can be seen in Fig. 15 below. Seen are two rosettes inter-connected, but very shallow (indicating either very early in formation or very slow growth rate). The rosette in the center has four out of six edges projecting lines; the reason for the missing rosette lines might be explained by the corresponding KPFM plot. There is a strong negative (blue) potential correlation to the rosette topography, but positive (red) potential spots are located where rosette lines would be expected. This would seem to indicate that there are differing defects competing with each other, and the topography is the indication of it.

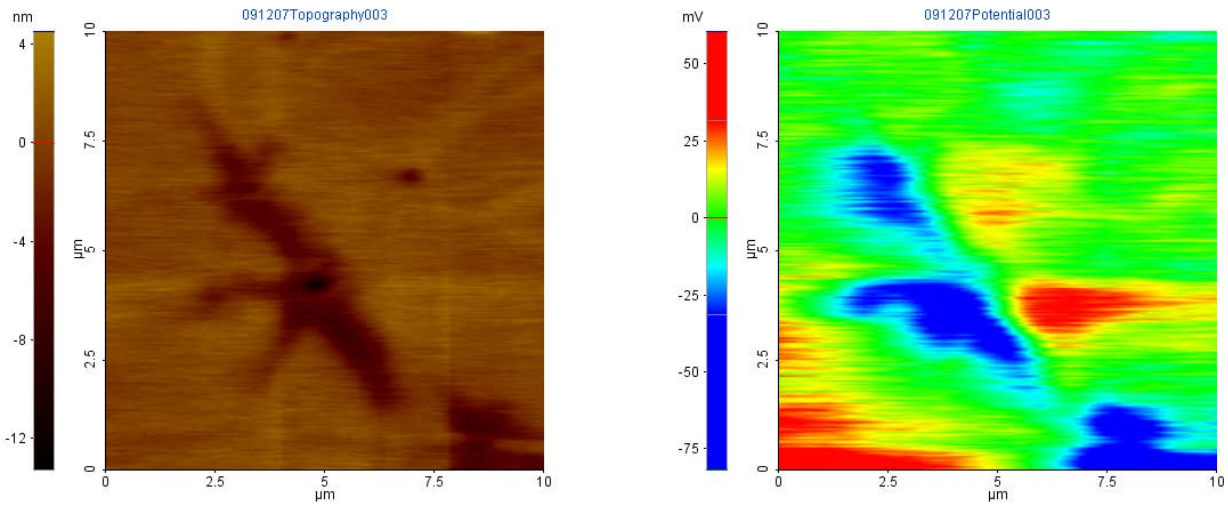

Figure 15 – Two Rosettes (AFM & KPFM, Zn face)

Several interesting energy states were found on the side-wall between two pits (see Fig. 16). The AFM and KPFM strongly correlate to each other (pits and blue potential spots), except for the rod/bump (AFM, white)—this is possibly a piece of dirt. An SPS plot taken at the interface between the pits reveals a large density of localized states below the bandgap with energy levels around 2.1 eV and 2.6 eV (Zn and O vacancies, respectively), among several other states. The large potential variation of this SPS was not confirmed with additional plots, but it is one of very few plots that show spectra that is stronger than the NBE (3.4 eV) spectra intensity. It would be expected for various defect states to be seen at such a point, as it is being affected by the growth process of a pit on both sides.

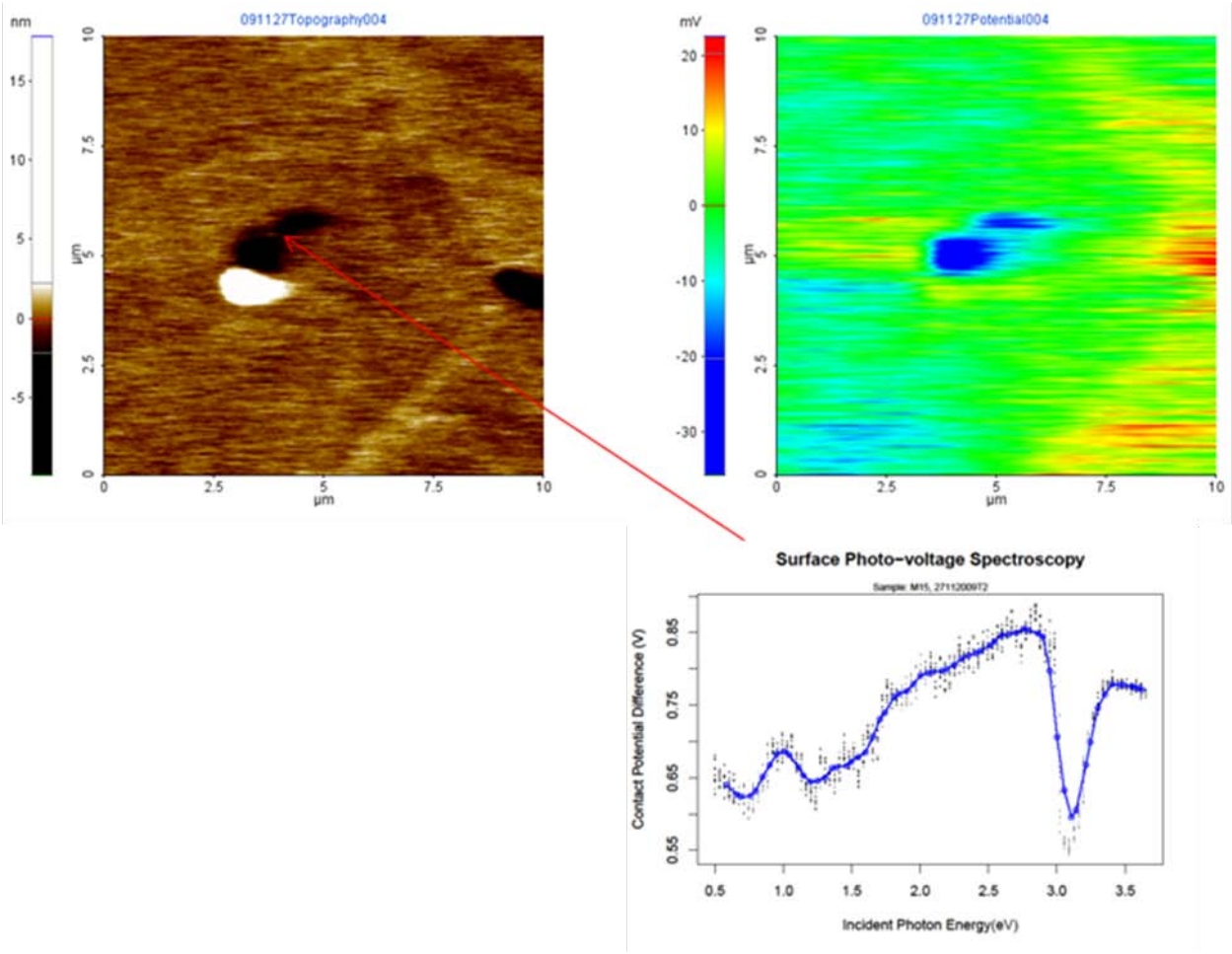

Figure 16 – Side-by-Side Pits (AFM & KPFM, SPS bottom-right, Zn face)

4.4 Other Relevant Work

Sample 2 showcases a lot of interesting nanofeatures on its surface. This is especially true due to the increased reactivity by oxygen plasma treatment that it underwent (see Fig. 17). The traditional pits can be seen, with lines of pits bending at 60º. Also evident is islanding—a very thin surface layer raised above the normal surface level (less than several nm)—which is not seen on sample one. The included green line profile shows that the trench of conjoined pits is not uniform in depth; it also shows that

the pits tend to have smooth slopes with the exception of several step edges possible; both properties are typical of pits conjoined into trenches as seen on sample one. Rosettes on this sample (not shown) also are very pronounced, more so than as seen on sample 1.

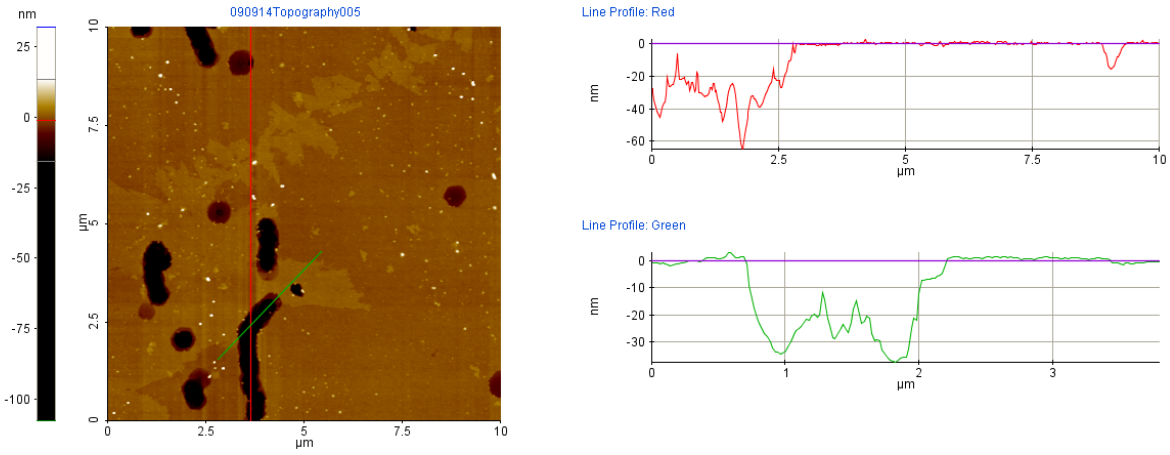

Figure 17 –Islanding and Pits (AFM, Zn face Sample 2)

Two sets of DR-CLS taken by co-researcher Dan Doutt help to confirm the polarity differences seen on ZnO. These spectra were taken on sample three. Fig. 18 clearly shows that a significant defect state exists on both faces; for Zn face, it exists around 2.45 eV (O vacancy) while for O face, it exists around 2.1 eV (Zn vacancy). As to be expected, the defect intensities are stronger below the surface. Interestingly on the Zn face, the weakest intensities are at both the lowest (0.1 keV) and highest (1 keV) incident electron beam energies, indicating that the defects are drawn to right below the surface; for the O face, the defects are doing the same but at a deeper location.

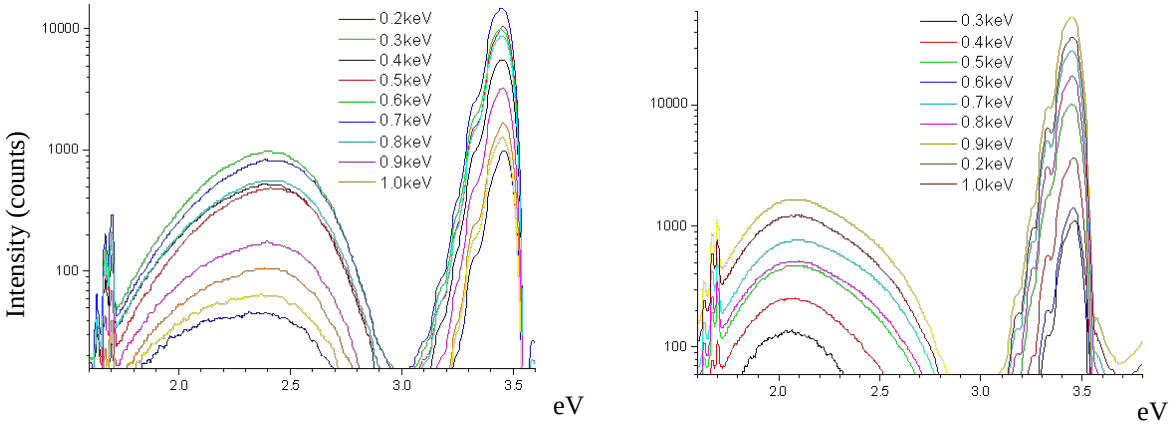

Figure 18 – DR-CLS of Zn face (left) and O face (right) (Sample 3) [Ref. D. Doutt, unpublished]

Some results in addition to co-researcher Tyler Merz's indicate that there is a distance relationship of defect states to nanofeatures. Doutt's SEM and DR-CLS, however, produce extremely sharp results that represent this, as can be seen in Fig. 19 below. Here, Doutt imaged a pit (with small bumps around its edge, possibly) and took DR-CLS at several points and graphed the ratio of NBE intensity to defect intensity (2.1 eV). As seen, the NBE intensity to defect intensity gets stronger, the farther the point is from the center of the pit (point 1), with the exception of point 4 which is on some bump feature, indicating that the defect states are decreasing with distance from the nanofeature. This then demonstrates that nanofeatures are associated with defect sites.

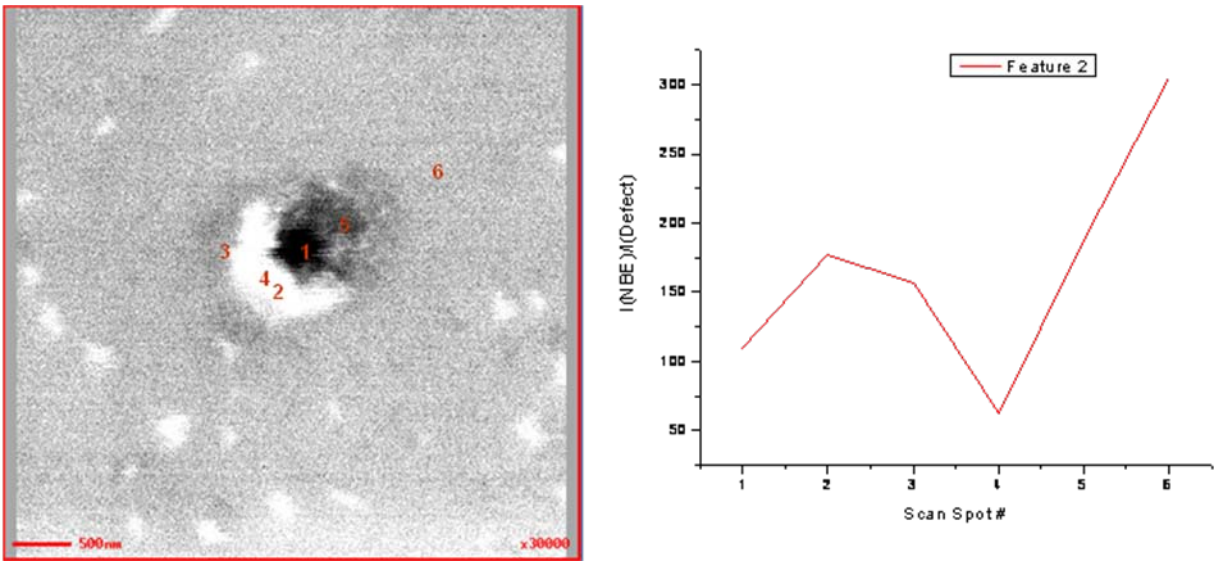

Figure 19 – SEM (left) and DR-CLS Intensities vs. Position (right)
(O face, Sample 3) [Doutt]

CHAPTER 5

CONCLUSIONS AND FUTURE WORK

5.1 Conclusions

It is imperative to consider surface characteristics when developing zinc oxide devices. This is because nanofeatures grow on it, in differing shapes and forms, depending on the polarity face. These surface nanofeatures grow spontaneously—sometimes in spontaneous locations, other times in patterns. To analyze the surface and features growing on it, tools such as AFM, KPFM, SPS, and DR-CLS are essential.

Oxygen face ZnO(000-1) is relatively strong in defects and impurities compared to the other face, zinc-terminated ZnO(0001). Oxygen face ZnO sees strong growth of nanorods, which can be seen in aligned rows that have corresponding surface potential; new rods develop along this invisible-topography line, visible-potential as well as other rods growing. Zinc face ZnO is characterized by pitting, including pits growing in alignment; close pits merge slowly into a trench. These polarities, then, affect the topographical growth characteristics: Oxygen face is more reactive, and it shows in how rods develop with seemingly low impurities or defects; the zinc atoms come from somewhere in the sample, with the possibility of oxygen atoms coming from the

atmosphere. Often times there is a correlation between the topography of these features and KPFM potential, indicating that there are surface states either aiding in the growth of the nanofeatures, or a resultant of the nanofeatures. If they do not have a correlation between topography and potential plots, it is possible that there are subsurface states involved that affect the topography, but are not measurable at the surface via KPFM.

Both faces see both features (rods and pits), as well as rosettes. What is different between the polarity faces is how the lines projecting from the center pit of the rosette can be either above-surface or below-surface, for oxygen- or Zinc face ZnO respectively. This matches the tendency for rods or pits, where Oxygen face is associated with growth above-surface and vice versa for Zinc face. This is not to say that pits don't grow on Oxygen face or the reverse for zinc, but that there is a strong, noticeable pattern. These rosette projection lines take on shallow depths or heights (typically several nanometers or less) and wide pathways (several hundred nanometers across); this would be ideal for mass transport of atoms, like a highway. The reason for the pathways is not understood, but could be explored as to their effect on the center pit's growth. Typically, these rosettes have a strong KPFM correlation showing that there are surface states involved with the surface features.

Also of significant note is the hexagonal characteristics taken up at the micro-level, stemming from ZnO's HCP crystal lattice structure. This can be observed in the well-defined hexagonal pits found on the Zinc face, or the 60º/120º angles between rosette projection lines and bends in trench lines. Only the pits on the zinc face have this strong hexagonal shape; rods on both faces and pits on the oxygen face do not exhibit

this. Hexagonal patterns allude to patterns following the most energetically-favorable method of growth due to the crystal structure, and thus nanofeatures would prefer to growth in this fashion. Why some nanofeatures do not grow in this favorable fashion is not understood.

The measurement techniques used in this paper all provide insight into the electronic characteristics of these surface nanofeatures. AFM is essential to mapping the topography and getting spatial and height information on the surface. KPFM is useful in observing the defect states that correlate with the surface topography and can be used to measure the surface work function influenced by these states. SPS provides insight, but seems limited at least with the first sample—possibly due to high sample quality and therefore low defect density—because while the plots show low noise and strong NBE emissions, the SPS response anticipated for the zinc and oxygen vacancy defect states are minimal compared to what has been reported elsewhere. This can stem from the difficulty in obtaining repeatable and low-noise plots; it is also possible it has to do with the non-uniformity of defect density around nanofeatures, as shown by on-going research by Tyler Merz. DR-CLS appears to be a better tool than SPS to gather defect density information at points, showing a strong peak at defect states for nanofeatures and in surrounding locations (as well as indicating a dependence on distance from the nanofeature).

The spontaneous growth of these nanofeatures continues to be spontaneous. That said, it is now clear that the face polarities significantly affect what surface nanofeatures grow, providing insight into the activity of the surface and subsurface states and their

related feature growth patterns. Zinc face ZnO exhibits strong features due to oxygen vacancies (n-type donors) and tends to pit, while Oxygen face has strong features due to zinc vacancies (p-type acceptors) and tends to grow nanorods. The HCP structure is also affecting the growth of features at some level, including rosettes which play a role in mass transport of atoms.

5.2 Future Work

As of the writing of this report, on-going research is being pursued on ZnO surface nanofeatures. One study is examining the stimulated mass transport spontaneous growth of nanofeatures by annealing these polar surfaces in an oxygen-rich furnace, studying the results from increasing temperature anneals on the surface. This anneal would simulate increased growth speed, as growth is exponentially dependent on temperature by way of the activation energy for the growth.

An important study that needs to be made, though, is one that attempts to answer the important question revolving upon which comes first: surface/subsurface defects or nanofeatures. This could be explored by picking a several sites with defects found by KPFM and SPS but no nanofeature correlation, sites with nanofeatures but no/minimal defect states found, and some with both—then examine the results after stimulated growth, looking at the contrast. This would be a challenging study since it means finding the same spots on the sample surface after repeated sample movements out of the AFM to perform annealing or other processes.

BIBLIOGRAPHY

[1] C. Klingshirn, "ZnO: Material, Physics and Applications," (pg. 782-803) ChemPhysChem 8, 2007.

[2] D. Doutt, H. L. Mosbacker, G. Cantwell, J. Zhang, J. J. Song, and L. J. Brillson, Appl. Phys. Lett. 94, 042111 2009.

[3] Y. Dong, F. Tuomisto, B.G. Svensson, A. Yu. Kuznetsov, and L.J. Brillson, "Vacancy Defect and Defect Cluster Energetics In Ion-implanted ZnO," Phys. Rev. B, Rapid Communications 81, 081201(R) (2010).

[4] Green, John-Bruce D., et al. "Modified tips: molecules to cells." Materials Today (Feb. 2003).

[5] Bustamante, Carlos and Keller, David. "Scanning Force Microscopy in Biology." Physics Today (Dec. 1995).

[6] Giessibl, Franz J. "AFM's path to atomic resolution." Materials Today (May 2005).

[7] Burgess, Daniel S. "Microscopy Probes Electron Behavior in Lasers." Photonics Spectra (July 2003); appeared earlier in *Applied Physics Letters* on June 9. 2003.

[8] Sahin. "High-resolution and large dynamic range nanomechanical mapping in tapping-mode atomic force microscopy." Nanotechnology 19.44 (2008): 445717.

[9] Nonenmacher, M. et al. "Kelvin Probe Force Microscopy." Appl. Phys. Lett. 58, 2921 (1991).

[10] Kronik, Leeor and Shapira, Yoram. "Surface Photovoltage Spectroscopy of Semiconductor Structuress: at the Crossroads of Physics, Chemisty and Electrical Engineering." Surf. Interface Anal. 31, 954 (2001).

[11] S. Lautenschlaege, et al. "Asymmetry in the excitonic recombinations and impurity incorportation of the two polar faces of homoepitaxially grown ZnO films." Phys. Rev. B 77 (2008), 144108.

[12] M. G. Wardle, et al. “First-Principles Study of the Diffusion of Hydrogen in ZnO.” Phys. Review Letters 96 (2006), 205504.